Structure and Dynamics of a Denatured 131-Residue Fragment of Staphylococcal Nuclease: A Heteronuclear NMR Study†

Andrei T. Alexandrescu, Chitrananda Abeygunawardana, and David Shortle*

Department of Biological Chemistry, The Johns Hopkins University School of Medicine, 725 North Wolfe Street, Baltimore, Maryland 21205

Received August 19, 1993; Revised Manuscript Received November 11, 1993®

ABSTRACT: A partially folded form of staphylococcal nuclease has been obtained by deleting residues 4–12 and 141–149 of the 149-residue wild-type protein. Sequence-specific NMR resonance assignments have been obtained for 106 of the 131 residues in this protein fragment by using multi-dimensional triple resonance NMR of samples enriched with ^{13}C and ^{15}N. Residues corresponding to helix 2 (residues 98–106) and helix 1 (residues 54–68) of the native state give chemical shifts and NOE effects characteristic of helical structure. These same residues, however, give coupling constants and NOE effects indicative of fast conformational averaging between helical and extended conformations. The residual helix structure observed in the nuclease fragment is thus considerably less persistent than the corresponding structure in the native state. Based on Hα chemical shifts, we estimate the fractional population of helical conformers to be 30% for helix 2 and 10% for helix 1. Two segments, 83–86 and 94–97, show NOE effects, coupling constants, and lowered amide temperature coefficients consistent with a native-like reverse-turn structure. The C-terminal α-helix as well as the fourth and fifth strands of the 5-strand β-barrel show little evidence for ordered structure. The first three strands of the β-sheet, part of the catalytic loop, and the first turn of helix 3 give significantly poorer NMR data than the rest of the protein, possibly as a result of exchange broadening, and could not be characterized in detail. That the most persistent elements of structure in the fragment are native-like suggests that nuclease may fold by a hierarchical mechanism.

In order to understand the rules of structure formation in proteins, it is desirable to have model systems with a level of conformational ordering intermediate between that of the fully folded and fully unfolded protein (Dobson, 1992a). Partially folded conformations have been observed for a number of proteins, both as transient kinetic intermediates during the folding reaction (Dobson, 1992b) and as partially folded conformations under equilibrium conditions (Baum et al., 1989; Kuwajima, 1989; Shortle & Meeker, 1989; Alexandrescu et al., 1993b; Shortle & Abeygunawardana, 1993; Stockman et al., 1993). Furthermore, the starting material for the folding reaction, which has long been assumed to be a "random coil", in some cases contains elements of ordered structure (Dill & Shortle, 1991; Dyson & Wright, 1991; Neri et al., 1992a,b; Alexandrescu et al., 1993). By examining residual structure in partially folded proteins at equilibrium, it may be possible to identify the most stable and independent units of structure and to then define the progression of structure assembly in a time-independent pathway (Shortle, 1993).

Given the complexity of the protein folding problem and the sparsity of information on partially folded proteins, structural characterizations of nonnative states generated by any means are of considerable interest. Site-directed mutagenesis, however, offers a relatively selective means of disrupting interactions in the native state. In the case of the denatured nuclease fragment that forms the subject of this paper, Δ131Δ,[1] the native state was destabilized by deleting 18 of the 149 residues in the full-length protein. The 18 residues deleted, 4–12 and 141–149, are at the flexible N- and C-termini of the chain and include 10 residues which are too disordered to give detectable electron density in the X-ray structure of the full-length protein (Loll & Lattman, 1989). Of the deleted residues, only L7 has a hydrophobic side chain. The reasoning behind this construct was to destabilize the native state[2] while maintaining the majority of residues involved in functionally important secondary and tertiary structure (Figure 1). A further advantage of characterizing denatured proteins generated by mutagenesis is that these can be studied near physiological conditions provided they are soluble and monomeric. This avoids the possibility of inducing a structure that is specific to a given solvent [e.g., Fan et al. (1993) and Alexandrescu et al. (1994)].

Δ131Δ retains wild-type enzymatic activity, which indicates the fragment is fully competent to refold to a conformation similar to that of the wild-type native state in the presence of high concentrations of substrate. Similarly, NMR and CD data suggest that Δ131Δ folds to a structure highly similar to that of the native state in the presence of the tight binding substrate analogue inhibitor pdTp (data not shown), a ligand known to strongly stabilize the native state (Shortle & Meeker, 1989). The Δ131Δ fragment has excellent solubility properties and has been shown to be monomeric by gel filtration experiments. The fragment can be efficiently overproduced

† This work was supported by NIH Grant GM34171 (D.S.).

* To whom correspondence should be addressed.

® Abstract published in *Advance ACS Abstracts*, January 15, 1994.

[1] Abbreviations: Δ131Δ, fragment of nuclease containing residues 1–3 and 13–140; ANS, 8-anilino-1-naphthalenesulfonate; CD, circular dichroism; $\Delta\delta/\Delta T$(HN), amide proton temperature coefficient; GuHCl, guanidinium hydrochloride; HMQC, heteronuclear multiple quantum correlation; HSQC, heteronuclear single quantum correlation; NMR, nuclear magnetic resonance; NOE, nuclear Overhauser enhancement; pdTp, thymidine 3′,5′-bisphosphate; RF, radio frequency; TOCSY, total correlation spectroscopy; TSP, 3-(trimethylsilyl)propionate-d_4. The nomenclature used to identify specific protons is that of the Brookhaven Protein Data Bank (PDB). The nomenclature for triple resonance scalar correlation experiments [e.g., HNCA, HN(CA)CO] is that of Kay et al. (1990).

[2] The N- and C-terminal deletions are each responsible for a decrease of approximately 4 kcal/mol in the stability of the native state to GuHCl denaturation, as measured by fluorimetric titrations using W140 as a probe.

0006-2960/94/0433-1063$04.50/0

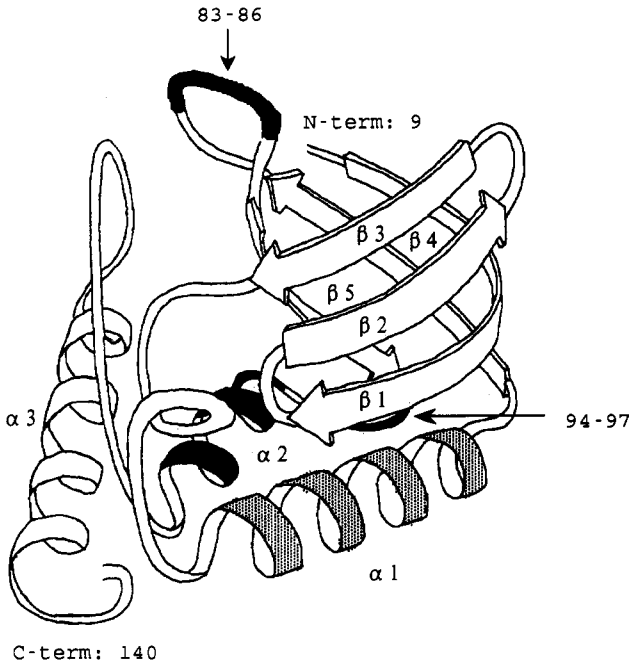

FIGURE 1: Ribbon diagram of native nuclease (copyrighted by Dr. Jane Richardson and used with her permission). The new N-terminus in Δ131Δ corresponds to residue 9 of the full-length protein; the new C-terminus corresponds to residue 140. The three α-helices (α1, 54–67; α2, 98–106; α3, 121–135), five strands of β-sheet (β1, 13–19; β2, 21–27; β3, 29–35; β4, 71–75; β5, 90–95), and two reverse turns (83–86 and 94–97) are labeled in the figure. The shaded regions indicate the elements of native-like residual structure identified in Δ131Δ (black, most persistent; gray, less persistent).

and isotopically enriched with ^{13}C and ^{15}N; typical yields are 40–60 mg/L of minimal media. Furthermore, the fragment can be purified to greater than 95% homogeneity if the purification steps are carried out in the presence of 6 M urea (Shortle & Meeker, 1989). The material purified by this procedure shows no evidence of significant degradation by proteolysis at room temperature for periods of days to weeks (as assayed by SDS–PAGE), a distinct advantage given the length of time required for the acquisition of multi-dimensional NMR data sets. These properties combine to make the Δ131Δ fragment an excellent model system for NMR studies of the denatured state of nuclease.

MATERIALS AND METHODS

Construction of Δ131Δ. The Kunkel (1985) modification of oligonucleotide-directed mutagenesis was applied to the wild-type nuclease gene cloned into phage vector M13mp9 to construct a deletion of codons 4–12 and to introduce a TAA stop codon at position 141. Each mutation was isolated separately and recombined into expression plasmid pL9 after sequencing the entire gene (Shortle et al., 1990). The double mutant gene was constructed by ligation of fragments using an internal *Hin*dIII site and then combined by fragment ligation into a pET11a T7 expression vector modified to contain codons 1–3 of staphylococcal nuclease, which includes a unique *Spe*I site (Shortle et al., 1990). The final gene encoded amino acids 1–3 and 13–140.

Sample Preparation. The gene for Δ131Δ was transformed into *Escherichia coli* strain HMS174 (DE3) (Novagen Inc., Madison, WI). Uniform enrichment with ^{15}N to a level >95% was obtained by growing 350-mL cultures of cells in MOPS media (Serpersu et al., 1986) supplemented with 0.5 g of $^{15}NH_4Cl$. To enrich to levels >95% with ^{13}C, an initial 100-mL culture was grown overnight in [^{12}C]glucose, and the cells from this culture were pelleted and resuspended in 350 mL of MOPS media supplemented with 1 g of [^{13}C]glucose. Nuclease expression was induced by making the culture 1 mM in isopropyl-β-thiogalactose when the A_{600} of the culture reached values of 1.5–2.0. In order to express the nuclease fragment, cells were incubated at 37 °C for an additional 4 h following induction.

Protein was purified by urea extraction, ethanol precipitation, and sulfo-Sepharose ion-exchange chromatography as described previously (Shortle & Meeker, 1989), except that a pre-extraction step of the harvested cells with 6 M urea, pH 9.2, without added NaCl was included. This step solubilizes almost all cellular proteins without solubilizing the nuclease fragment present in inclusion bodies. After dialysis against deionized H_2O, the isolated protein was lyophilized and stored as a powder at −70 °C. The Δ131Δ samples used for NMR were ≥95% pure by SDS–PAGE.

CD Spectroscopy. Spectra were collected on a AVIV-DS60 instrument in a 0.1-mm path length cell thermostated at 32 °C. Protein concentrations were 1 mg/mL in a 10 mM sodium acetate buffer, pH 5.3. For each spectrum, five scans collected at 0.5-nm increments were averaged, smoothed, and subtracted from the spectrum of the same cuvette filled with buffer.

NMR Spectroscopy. All heteronuclear NMR experiments were done on two samples of Δ131Δ: a ^{15}N-labeled sample and a ^{15}N,^{13}C double-labeled sample. Unless otherwise indicated, all NMR data were collected on samples at pH 5.3 and a temperature of 32 °C. The NMR solutions contained no added buffers or salts.

NMR spectra were collected at 600 MHz on a Bruker AM600 instrument at Johns Hopkins, except for a 2D ^1H-{^{15}N}HSQC-*J* and 3D ^1H{^{15}N}HSQC-NOESY-HSQC collected on a AM600 at NMRFAM in Madison, WI. All heteronuclear experiments were collected with the instruments operating in "reverse" mode. In HSQC-based experiments, the solvent resonance was suppressed by short 1.5-ms spin-lock pulses (Messerle et al., 1989). In all other experiments, water suppression was achieved by presaturation with a DANTE pulse sequence (Kay et al., 1989). Proton chemical shifts are reported with respect to an internal TSP reference standard; carbon chemical shifts are reported with respect to an external standard of TSP in D_2O (0.0 ppm at 32 °C). Nitrogen chemical shifts are reported with respect to an external standard of 2.9 mM $^{15}NH_4Cl$ in 1 M HCl at a temperature of 20 °C, which corresponds to a value of 24.93 ppm downfield of liquid ammonia (Levy & Lichter, 1979).

The 2D ^1H{^{15}N}HSQC (Bax et al., 1990); 3D ^1H{^{15}N}-NOESY-HMQC; TOCSY-HMQC (Marion et al., 1989a); and 3D HNCA, HNCO, HCACO (Kay et al., 1990), HN-(CO)CA (Bax, & Ikura, 1991) data sets were collected according to previously published procedures. A 3D ^1H{$^{13}C\alpha$}-NOESY-HMQC was collected in a similar fashion to that described for 3D ^1H{^{13}C}NOESY-HMQC (Gronenborn et al., 1989) except that a 90° ^{13}C pulse of 98 μs (corresponding to an RF field strength of 2.5 kHz) was used for selective excitation of Cα carbons. The mixing time for the TOCSY-HMQC experiment was 70 ms; mixing time for NOESY-HMQC and HSQC-NOESY-HSQC experiments was 200 ms. Data matrix sizes, spectral windows, and digital resolution in processed data sets are given in the supplementary material.

Amide proton temperature coefficients [$\Delta\delta/\Delta T$(HN)] were determined from ^1H{^{15}N}HSQC data sets collected at 32, 37, 42, and 47 °C. In order to determine $^3J_{HN\text{-}H\alpha}$ coupling constants, a ^1H{^{15}N}HMQC-*J* spectrum was collected using method 3 of Kay and Bax (1990).

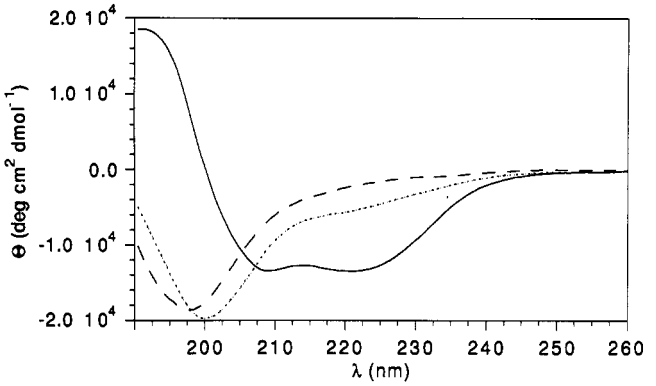

FIGURE 2: Far-ultraviolet CD spectra of full-length wild-type nuclease (solid line), Δ131Δ (dotted line), and tryptic digest of Δ131Δ (dashed line). The tryptic digest of Δ131Δ was obtained by incubating a 1 mg/mL solution of the protein in the presence of 10 μg/mL bovine-TPCK trypsin for 1.5 h at 37 °C.

Data Processing. NMR data were processed using the FELIX 1.1–2.1 software packages on IRIS and INDIGO Silicon Graphics computers. A convolution of the time domain data (Marion et al., 1989b) was usually applied to diminish the intensity of the residual solvent signal. 2D $^1H\{^{15}N\}$HSQC spectra were resolution enhanced by 30° shifted sine bell and sine bell squared functions in the t2 and t1 dimensions, respectively, and were zero-filled 1–2 times before Fourier transformation. The 3D data sets were zero-filled at least once in each dimension. The t3 dimension was resolution enhanced by multiplying with a 90° shifted sine bell; the t2 dimension was processed with a sine bell squared function with a 60–90° shift. The t1 dimension was extended by one-third of the original size using the forward linear prediction routine in FELIX, followed by attenuation by a 60–90° shifted sine bell squared function.

The t1 and t2 dimensions of 3D matrices often do not contain sufficient resolution to permit precise measurements of chemical shifts. In order to obtain more precise values, the 1D vectors of each 3D cross-peak along the t1 (x, 0, z) and t2 (x, y, 0) dimensions were processed further. A Hilbert transformation was applied to the 1D vector, followed by an inverse Fourier transformation, zero-filling to 1024 or 2048 data points, and a Fourier transformation. We found that the chemical shifts of the same nuclei in different experiments (e.g., C′ in HCACO and HNCO) showed much better agreement when this procedure was used rather than simple peak-picking of cross-peaks in 2D planes.

In order to determine $^3J_{HN\text{-}H\alpha}$ coupling value, the doublet components in the ^{15}N dimension was simulated by Lorentzian lines using the peak-fitting routine in FELIX 2.1. The peak height, line width, and doublet separation were optimized manually during the fitting procedure in order to give the best agreement between the experimental and simulated data. Amide temperature coefficients were measured as the slopes of the linear variation of HN chemical shifts with temperature.

RESULTS

CD Spectroscopy. Figure 2 compares the far ultraviolet CD spectra of full-length wild-type nuclease Δ131Δ and a tryptic digest of Δ131Δ. The CD traces indicate that Δ131Δ has more secondary structure than the sum of its tryptic fragments, but considerably less than the wild-type protein. Based on the observed ellipticity at 222 nm, we estimate that the α-helix content of Δ131Δ is 25–30% that of the full-length native protein. This is in marked contrast to the "molten globule" class of partially folded proteins which typically exhibit peptide CD spectra similar in shape and magnitude to their corresponding native states (Kuwajima, 1989). These spectra suggest that Δ131Δ represents a partially folded protein with much less residual structure than a molten globule, consistent with the NMR properties of this fragment (see below).

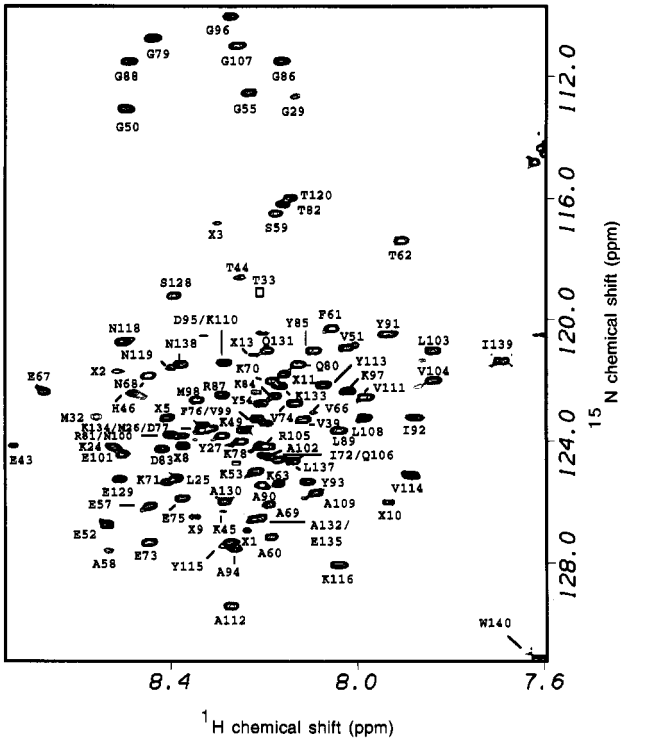

FIGURE 3: 2D $^1H\{^{15}N\}$HSQC spectrum of Δ131Δ at pH 5.3 and 32 °C. The H–N cross-peaks are labeled according to the sequence-specific assignments (supplementary material). Peaks marked "X" have not been assigned. The cross-peak assigned to T33 can only be seen at lower contour levels.

Backbone Amide Resonances. Figure 3 shows a 2D $^1H\{^{15}N\}$HSQC spectrum of Δ131Δ. Of the expected 126 backbone amide cross-peaks, excluding five proline residues in the sequence of Δ131Δ, 105 backbone amide cross-peaks could be detected in this spectrum. As shown in Figure 3, there is significant variability in the intensities of the cross-peaks. For example, of the nine glycine peaks expected from the sequence of Δ131Δ, only eight could be detected, and one of these, G29 (8.13, 112.72 ppm), gives a significantly weaker peak. In 2D ^1H-NMR spectra (COSY, NOESY) of Δ131Δ, the aromatic proton resonances of the three Phe, three His, and seven Tyr residues show little dispersion, and no resonances were detected upfield of 0.76 ppm (data not shown). The backbone amide proton resonances occur between 7.6 and 8.7 ppm. By contrast, the corresponding resonances in the full-length native protein span a range between 6.2 and 10.6 ppm (Wang et al., 1992). The N chemical shift dispersion (110–131 ppm), however, shows a relatively small decrease compared to that of the native protein (103–137 ppm). Good nitrogen chemical shift dispersion has been observed in other denatured proteins (Neri et al., 1992; Logan et al., 1993; Shortle & Abeygunawardana, 1993; Stockman et al., 1993; van Mierlo et al., 1993) and presumably reflects the insensitivity of backbone nitrogen chemical shifts to conformation-dependent effects (Wishart et al., 1991).

Resonance Assignment by Residue Type. Spin systems were classified according to residue type using primarily scalar coupling information from a 3D $^1H\{^{15}N\}$TOCSY-HMQC experiment. Because Δ131Δ gives relatively sharp lines, it

was possible to obtain good signal/noise in a $^1H\{^{15}N\}$TOCSY-HMQC with a relatively long mixing time of 70 ms. In many cases, magnetization transfer was observed from side-chain protons as far away as γ or δ protons to the backbone amide proton (supplementary material). A practical advantage in obtaining residue-type NMR assignments for Δ131Δ is that conformation-induced chemical shifts are smaller than in native proteins; consequently, side-chain chemical shift values better approximate those of free amino acids. Amide protons were provisionally classified according to residue type by using a strategy similar to that of Redfield and Dobson (1988). The group of residues "J" (Asp, Asn, Ser, His, Trp, Tyr, Phe) give characteristic β-proton chemical shifts downfield of 2.3 ppm; the group of residues "U" (Val, Glu, Gln, Lys, Arg, Met, Ile, Leu, Val) give characteristic β-proton chemical shifts upfield of 2.3 ppm. Ala and Thr give strong methyl proton cross-peaks at 1.4–1.2 ppm. A number of other subclassifications were possible; the methyl-containing U residues (Val, Ile, Leu) give rise to TOCSY methyl proton connectivities near 1.0–0.8 ppm, but Val has a distinctive β-proton chemical shift of 2.1–1.9 ppm; Phe and Tyr residues could often be distinguished from other J-type spin systems based on weak NOEs to δ aromatic protons near 7.0 ppm; Gly residues give characteristic N chemical shifts near 110 ppm and $^{13}C\alpha$ chemical shifts near 45 ppm in HNCA and HN(CO)CA experiments. The disparate group of residues (Pro, Val, Ile, and Thr) all give $C\alpha$ chemical shifts larger than 60 ppm in Δ131Δ. Of the 105 cross-peaks detected in the $^1H\{^{15}N\}$HSQC experiment, 90 could be grouped into one of the classes above.

Sequence-Specific Assignments. The classical approach for obtaining sequence-specific NMR resonance assignments is to link spin systems via $d_{NN}(i,i+1)$ and $d_{\alpha N}(i,i+1)$ through-space NOE connectivities (Wüthrich, 1986). Sequential assignments via NOE connectivities are complicated considerably, however, in cases where the chain folds back on itself. To obtain sequential assignments for Δ131Δ, we used the experiments originated by Kay et al. (1990), which establish through-bond sequential connectivities via scalar heteronuclear magnetization transfer. The HNCA and HN(CO)CA experiments provide one pathway for sequential connectivities. The HNCA experiment connects each H–N cross-peak with its own $C\alpha$ chemical shift and in most cases with that of the preceding $C\alpha$ (supplementary material). The one-bond coupling constant connecting $N(i)$ and $C\alpha(i)$ has a magnitude of 7–11 Hz while the two-bond coupling constant connecting $N(i)$ and $C\alpha(i-1)$ has a magnitude of 5–8 Hz (Kay et al., 1990). This gives the HNCA experiment directionality; the intraresidue connectivities are almost always stronger than the interresidue connectivities. The two types of connectivities can be distinguished unambiguously in the HN(CO)CA experiment which only detects the interresidue connectivity.

The combined use of the 3D HNCO and HCACO experiments provides a second independent pathway for obtaining scalar sequential connectivities. The HCACO experiment establishes a correlation between each $H\alpha$–$C\alpha$ pair and the C′ resonance of the same residue. The HNCO experiment provides sequential information by connecting each H–N pair with the C′ resonance of the preceding residue. In the case of the Δ131Δ fragment, however, $H\alpha$ and $C\alpha$ dispersion is much poorer than that of HN and N resonances. The HCACO experiment, in contrast to the experiments above, also has the disadvantage of only providing intraresidue connectivities. Thus, residue types are well-separated from each other (e.g., Gly from Thr), but in the common case where spin systems of the same type have similar $H\alpha$, $C\alpha$, and C′ chemical shifts (e.g., G29, G55, G96, G107), the overlap for amino acids of the same type severely complicates assignments. These factors made the HCACO/HNCO sequential assignment pathway less useful than the HNCA/HN(CO)CA pathway. While the HCACO/HNCO provided confirmation for some of the assignments obtained from the HNCA/HN(CO)CA experiments, no new assignments were obtained by this method.

A large number of $H\alpha(i)$–$NH(i+1)$ and $H\beta(i)$–$HN(i+1)$ NOEs could be identified for Δ131Δ. These through-space NOE correlations provided further independent confirmation of the sequence-specific assignments. The interresidue HNCA/HN(CO)CA, HCACO/HNCO, and $H\alpha(i)$–$HN(i+1)$ and $H\beta(i)$–$HN(i+1)$ NOE connectivities observed in Δ131Δ are summarized in the supplementary material.

Of the 105 backbone amide peaks detected in the 2D $^1H\{^{15}N\}$HSQC experiment, 93 could be assigned (Figure 3). Additional C′, $C\alpha$, $H\alpha$, and side-chain protons resonance assignments could be obtained for another 13 residues, based on HNCO and/or HNCA/HN(CO)CA coupling information. In total, sequence-specific resonance assignments were obtained for 106 of the 131 residues in the Δ131Δ fragment (see supplementary material). The regions of the fragment for which no assignments could be obtained include 12 of the first 13 residues at the N-terminus; residues 34–37, one of the most hydrophobic segments of the molecule; residues 40–41, part of the catalytic loop; and residues 121–126, the first turn of helix 3. Of the assigned residues in the N-terminal third of Δ131Δ, residues E43–H46 and G29–T33 give some of the weakest cross-peaks in the $^1H\{^{15}N\}$HSQC experiment. Similarly, most of the 12 cross-peaks that could not be assigned in the $^1H\{^{15}N\}$HSQC spectrum are weak, which is primarily responsible for the lack of progress in assigning the N-terminal region of the molecule.

Chemical Shift Indices. The chemical shift is one of the easiest and most accurately measured NMR parameters. The lack of a good theoretical foundation for understanding conformational contributions to chemical shifts has, however, limited the use of these data in protein structure determination. Nevertheless, strong empirical correlations have been observed between chemical shift values and secondary structure in proteins (Spera & Bax, 1991; Wishart et al., 1991). In native proteins, $C\alpha$ resonances are the most sensitive to secondary structure, followed by $H\alpha$ and C′ resonances, while the HN and N nuclei are relative insensitive probes (Wishart et al., 1991). For $H\alpha$, HN, and N, positive differences (downfield shifts) from random coil values correlate with β-sheet structure while negative differences (upfield shifts) correlate with α-helix structure (Wishart et al., 1991). The $C\alpha$ and C′ chemical shifts show the opposite sign dependence.

Figure 4 plots chemical shift differences

$$(\Delta131\Delta) - (\text{coil}) \quad (1)$$

for the $C\alpha$, C′, and $H\alpha$ resonances. The HN and $H\alpha$ proton random coil values were obtained from Gly–Gly–X–Ala model peptides (Wüthrich, 1986). No comparable values are available for N, $C\alpha$, and C′ nuclei. For these resonances, the "coil" values given in Wishart et al. (1991) were used. These values were calculated from a database of chemical shifts for residues found to be in regions of nonregular secondary structure (coil) in native-state X-ray structures. All of the nuclei analyzed in Δ131Δ show differences in the means from these coil values. The mean difference over all residues is 2.73 ppm for N, 1.71 ppm for C′, and 1.45 ppm for $C\alpha$. The corresponding values for $H\alpha$ are –0.03 ppm when the peptide

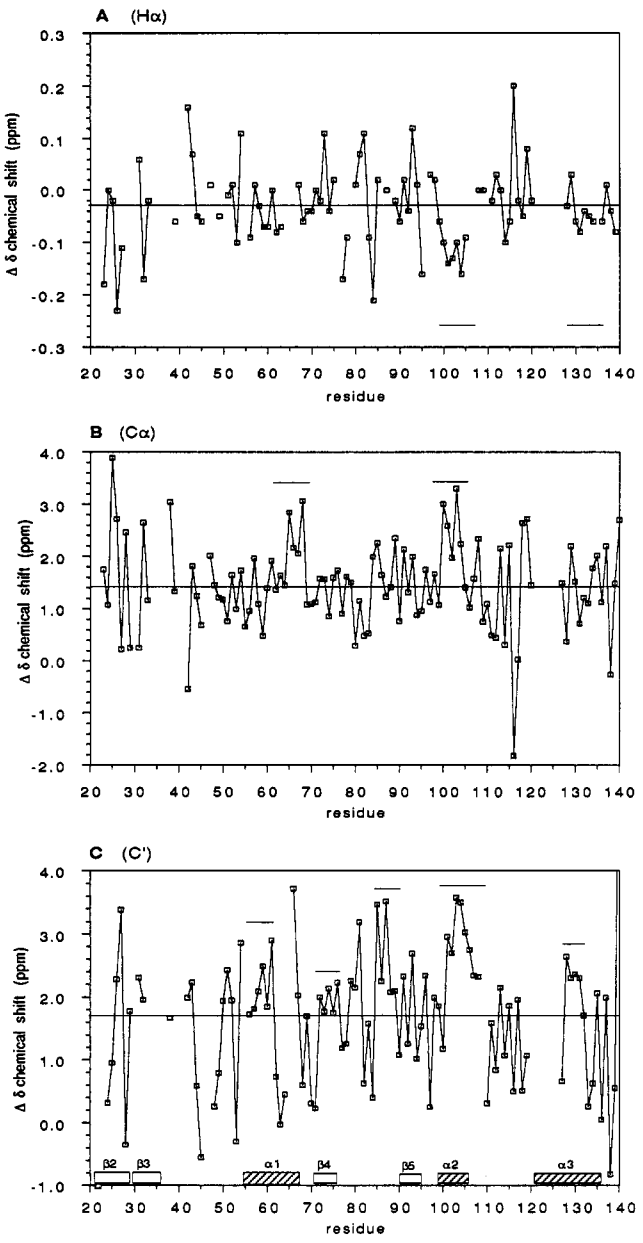

FIGURE 4: Chemical shift indices for Δ131Δ. (A) Hα protons; (B) Cα carbons; (c) carbonyl carbons. The horizontal baseline is drawn through the mean of the chemical shift difference for each nucleus. This value differs from zero due to calibration offsets, and possibly as a result of conformational differences between unstructured coils in solution and coil conformations in X-ray structures (see text). Regions of the sequence which give α-helix and β-sheet structure in the native state are summarized in panel C. The thin horizontal lines indicate stretches of residues which show chemical shift deviations characteristic of the α-helix structure in Δ131Δ.

values (Wüthrich, 1986) are used and 0.08 ppm when the folded coil values (Wishart et al., 1991) are used. The differences observed for N, C′, and Cα may arise from calibration offsets in this work or in the database. Thus the coil Cα chemical shifts reported by Spera and Bax (1991) have a mean offset of 1.15 ppm downfield from those of Wishart et al. (1991). The Hα resonances, however, can be accurately calibrated against the internal reference standard TSP. The poorer agreement between Δ131Δ and coil values derived from crystal structures indicate that the latter may not be as appropriate as peptide models for describing disordered proteins. In particular, the chemical shift values of residues not involved in regular structure in native proteins may be influenced by additional factors of the rigid native-state structure, such as local magnetic anisotropy, ring current effects, and restricted mobility.

A convenient cutoff for analyzing Δ131Δ chemical shift deviations in terms of secondary structure is a stretch of five residues with uninterrupted positive or negative differences from the mean (e.g., 1.45 ppm for Cα). The strongest trends are observed for residues which occur in helix 2 (98–106) in the native structure; residues in this region give strong helix-like chemical shifts for all three indices. Residues from helix 1 (54–67) give helix-like shifts for the Cα and C′ indices, while residues from helix 3 (121–135) give helix-like shifts for the Hα and C′ indices. None of the indices gave patterns indicative of β-sheet structure. The conformationally insensitive N and HN nuclei give no clear patterns of either α-helix or β-sheet shifts (not shown).

NOESY Spectroscopy. The amide protons in 3D $^1H\{^{15}N\}$-NOESY-HMQC spectra of Δ131Δ show primarily intraresidue NOE correlations and NOE correlations to protons of the preceding residue in the sequence. For the majority of cases where both types of effects could be observed, the magnitude of $d_{\alpha N}(i,i+1)$ NOE was the same or larger than that of the $d_{\alpha N}(i,i)$ NOE. This is expected for residues in the extended β-region of φ, ψ space (Wüthrich, 1986) and is commonly observed for unstructured peptides (Dyson & Wright, 1991).

A number of residues show $d_{NN}(i,i+1)$ NOEs in the $^1H\{^{15}N\}$NOESY-HMQC spectra of Δ131Δ. Additional $d_{NN}(i,i+1)$ and $d_{NN}(i,i+2)$ NOEs could be identified in a $^1H\{^{15}N\}$HSQC-NOESY-HSQC spectrum (data not shown) for some of the HN protons which were unresolved in the 3D $^1H\{^{15}N\}$NOESY-HMQC. Strong $d_{NN}(i,i+1)$ NOEs are associated with either turn or α-helix conformations. Some of the strongest $d_{NN}(i,i+1)$ NOEs connect the stretch of residues 99–105, which form helix 2 in the native structure (Figure 5). Additional regions of the sequence which give strong $d_{NN}(i,i+1)$ NOEs are residues 85–86 and 96–97, reverse turns in the native structure.

The identification of nonsequential $d_{NN}(i,i+2)$, $d_{\alpha N}(i,i+2)$, $d_{\alpha N}(i,i+3)$ NOEs provides strong evidence for helix or turn structure. As stated above, most of the HN protons in Δ131Δ give strong $d_{\alpha N}(i,i)$ and $d_{\alpha N}(i,i+1)$ NOEs. The small magnitude of the medium range NOEs coupled with the very small Hα chemical shift dispersion in Δ131Δ made the analysis of $d_{\alpha N}(i,i+2)$, $d_{\alpha N}(i,i+3)$, and $d_{\alpha N}(i,i+4)$ NOEs extremely difficult. In order to identify these types of NOEs, each resolved t2 HN vector of the processed 3D NOESY-HMQC spectrum was additionally processed to provide better resolution by the procedure described in the Experimental Section. Despite extensive efforts to increase Hα resolution by data processing, however, the presence or absence of $d_{\alpha N}(i,i+2)$ could not be ascertained for 59 of the 91 assigned HN vectors in Δ131Δ due to overlap of one of the resonances in this pair. Similar problems were encountered in the analysis of $d_{\alpha N}(i,i+3)$ and $d_{\alpha N}(i,i+4)$ NOEs. The $d_{NN}(i,i+2)$, $d_{\alpha N}(i,i+2)$, and $d_{\alpha N}(i,i+3)$ that could be identified occur primarily in the regions of the sequence which correspond to the first and second helices. Residues 83–86 and 94–97, reverse turns in the native state, also give $d_{NN}(i,i+2)$ and $d_{\alpha N}(i,i+2)$ correlations.

The $d_{\alpha\beta}(i,i+3)$ NOE is highly characteristic of helical structure in native proteins (Wüthrich, 1986). In order to identify these types of NOEs, we employed a variant of the 3D $^1H\{^{13}C\}$NOESY-HMQC spectrum in which the Cα subset of aliphatic carbon resonances was selectively excited [3D $^1H\{^{13}C\alpha\}$NOESY-HMQC]. With the exception of resonances from glycine residues, there are no Cα resonances in Δ131Δ

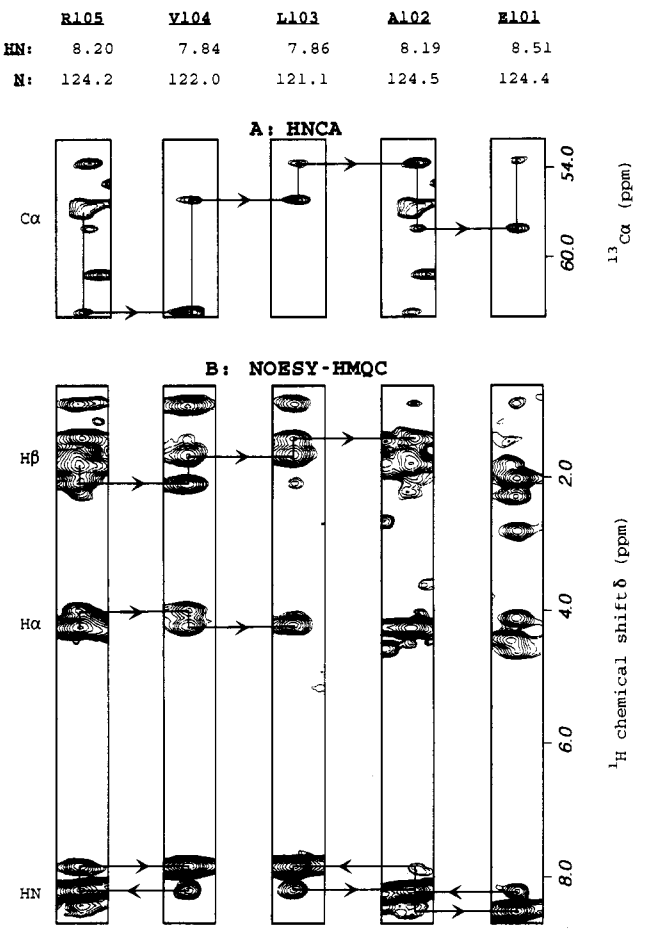

FIGURE 5: NOE and HNCA strips for residues R105–E101 of Δ131Δ. (A) Strips from the 3D HNCA data set that illustrate the conformation-independent assignments for this sequence. (B) Strips from the 3D ^{1}H{^{15}N}NOESY-HMQC data set. The resolvable $d_{NN}(i,i+1)$, $d_{\alpha N}(i,i+1)$, and $d_{\beta N}(i,i+1)$ correlations are indicated in the figure. An additional $d_{NN}(103,104)$ correlation could be resolved only in a 3D ^{1}H{^{15}N}HSQC-NOESY-HSQC experiment (not shown). The HN and N coordinates for each 2D strip are given at the top of the figure.

upfield of 52 ppm or downfield of 64 ppm. This made it possible to set a much narrower sweep width for Cα (44–66 ppm) than would have been possible in a conventional 3D ^{1}H{^{13}C}NOESY-HMQC. Nevertheless, significant overlap is still a problem for residues with nondistinct Cα and Hα chemical shifts: Leu, Lys, Arg, Gln, and Glu. The presence or absence of $d_{\alpha\beta}(i,i+3)$ could not be ascertained for 57 of the 97 assigned HCα vectors in Δ131Δ due to the overlap of one of the pair of resonances in the $\alpha(i)$, $\beta(i+3)$ pair. The vast majority of interpretable Hα resonances show only intraresidue NOEs. Only six $d_{\alpha\beta}(i,i+3)$ NOEs were identified in Δ131Δ, three occur in the first helix and three in the second helix of native nuclease (Figure 6). It is worth noting that the resolution of these NOEs was facilitated somewhat by the Hα and Cα chemical shift perturbations experienced by these residues (Figure 4).

In native proteins $d_{\alpha\alpha}(i,j)$ NOEs are characteristic of β-sheet structure (Wüthrich, 1986). Only two pairs of residues connected by $d_{\alpha\alpha}(i,j)$ NOEs were found in Δ131Δ. One weak NOE connects the Hα of H46 (the most downfield Hα resonance at 5.04 ppm) to the Hα of P47 at 4.45 ppm. The second $d_{\alpha\alpha}$ NOE (4.33 ppm, 4.55 ppm) could not be identified.

HN Temperature Factors and $^3J_{HN\text{-}H\alpha}$ Coupling Constants. Amide proton temperature coefficients [$\Delta\delta/\Delta T$ (HN)] are believed to reflect the hydrogen-bonding state of amide protons;

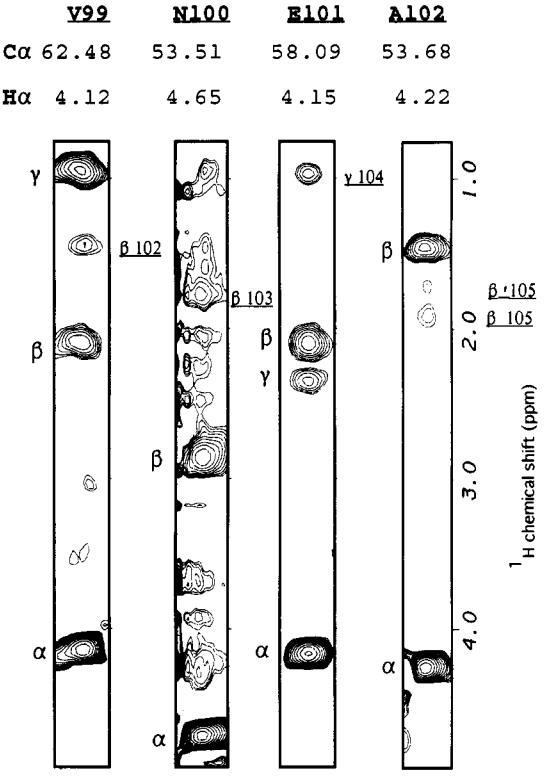

FIGURE 6: Strips from a 3D ^{1}H{^{13}Cα}NOESY-HMQC illustrating $d_{\alpha\beta}(i,i+3)$ correlations for residues V99–A102 in Δ131Δ. The Cα and Hα coordinates for each 2D strip are given at the top of the figure. The labels on the left of each strip denote intraresidue connectivities; the labels on the right of each strip denote $d_{\alpha\beta}(i,i+3)$ interresidue connectivities. The $d_{\alpha\beta}(101,104)$ connectivity could not be established because the β-protons of E101 and V104 have degenerate chemical shifts. A medium intensity $d_{\alpha\gamma}(101,104)$ correlation observed for these residues, however, is consistent with the native-state structure d = 3.8 Å. An additional weak $d_{\alpha\beta}(104,108)$ correlation (not shown) is also likely to be related to α-helix structure in this segment.

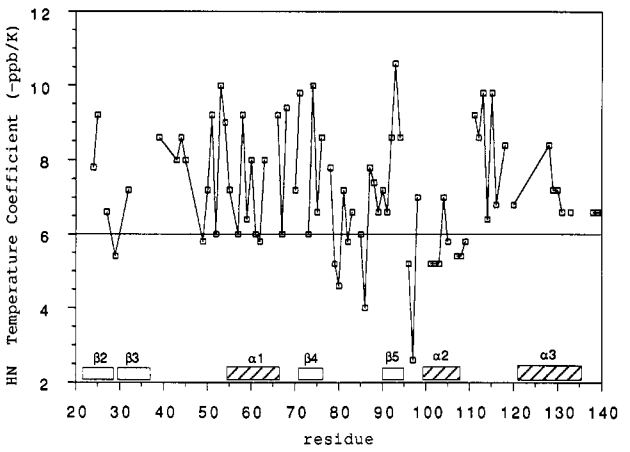

FIGURE 7: Amide proton temperature coefficients for Δ131Δ. Values greater than 6.5 ppb/K are characteristic of non-hydrogen-bonded conformations.

these are sensitive to hydrogen-bonded conformations which are too short-lived to give measurable protection from hydrogen exchange (Dyson & Wright, 1991). A lowered [$\Delta\delta/\Delta T$(HN)] is indicative of an increased fraction of hydrogen-bonded conformations. In Δ131Δ, small $\Delta\delta/\Delta T$ (HN) values occur primarily in the second helix and to some extent in the first helix (Figure 7). The fourth positions of the 83–86 and 94–97 turns show some of the smallest $\Delta\delta/\Delta T$ (HN) values; the third position in both turns also shows lowered values.

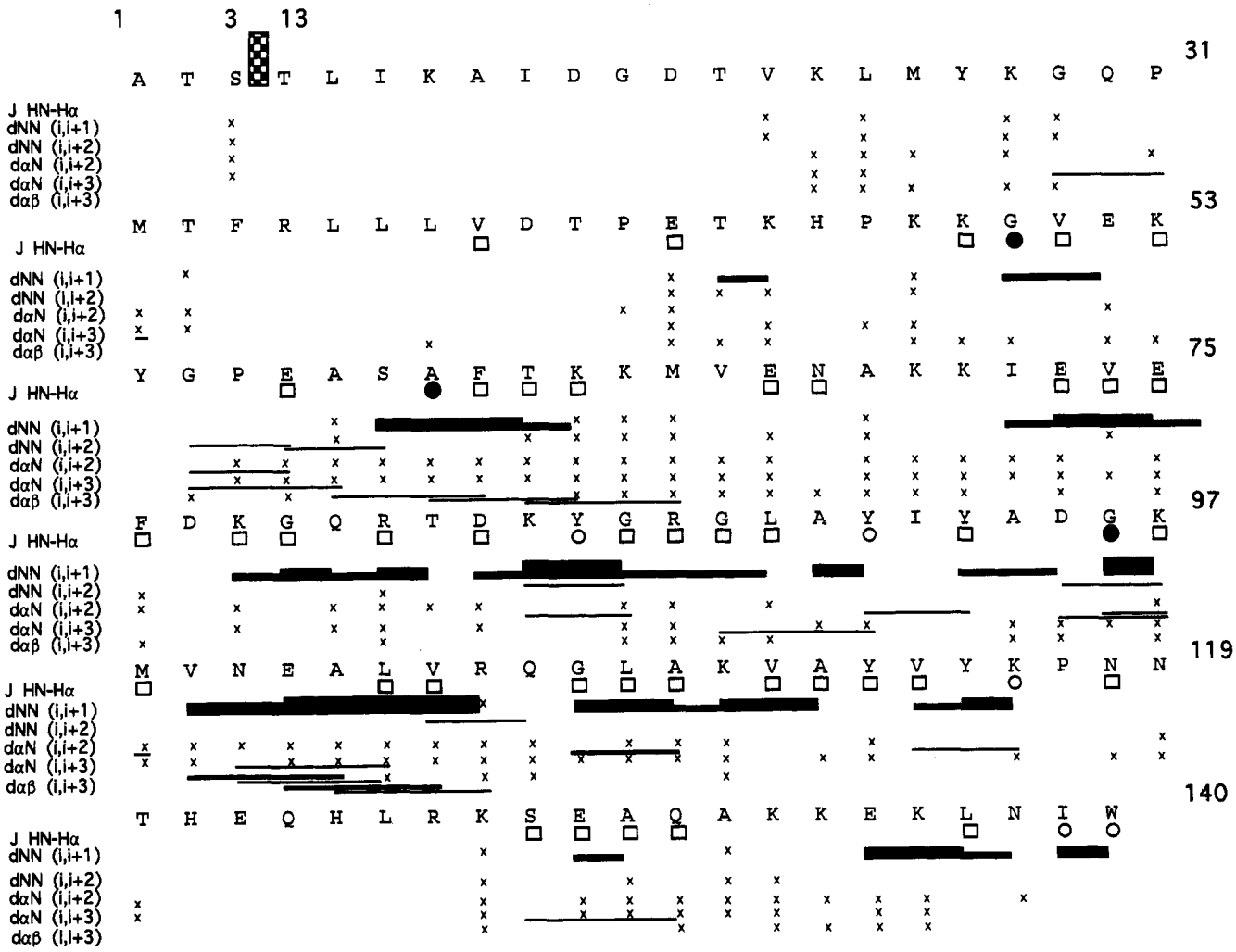

FIGURE 8: NMR parameters related to secondary structure in Δ131Δ. The open boxes indicate $^3J_{HN\text{-}H\alpha}$ coupling constants between 6.5 and 8.5 Hz. Filled circles indicate coupling constants below 6.5 Hz; open circles denote coupling constants above 8.5 Hz. The thickness of the horizontal bars denote the intensities of the NOEs. The intensities of the $d_{\alpha N}(i,i+1)$ NOEs, which are not given in this figure, were uniformly strong to medium. The letter "x" indicates that NOE connectivity information could not be obtained because of overlap, weak signals, or lack of assignments.

The $^3J_{HN\text{-}H\alpha}$ coupling constants measured from HMQC-*J* spectra of Δ131Δ are summarized in Figure 8. The vast majority of these (83%) have values between 6.5 and 8.5 Hz and, thus, suggest extensive motional averaging (Dyson & Wright, 1991). Five residues give $^3J_{HN\text{-}H\alpha}$ coupling values greater than 8.5 Hz, one of these is residue Y85 (8.8 Hz), the third position in the native 83–86 turn. Only two residues give $^3J_{HN\text{-}H\alpha}$ values less than 6.5 Hz: G96 (5.8 and 5.9 Hz), the third position of the native 94–97 turn, and A60 (5.4 Hz) in the first helix. The $^3J_{HN\text{-}H\alpha}$ coupling constant data and short-range NOE data for Δ131Δ are summarized in Figure 8.

DISCUSSION

α-Helix Structure and Dynamics. Two of the three segments which form α-helices in the native state show evidence (Figure 8) for helical structure in the Δ131Δ fragment. At the same time, these same residues also show clear evidence of averaging between helical and extended conformations [strong $d_{\alpha N}(i,i+1)$ NOEs and coupling constants near 7 Hz]. The helical and extended conformations are in fast exchange on the chemical shift time scale since each of the amide protons in Δ131Δ gives only one resonance. Based on these observations and differences from "random coil" chemical shift values of Hα protons in helical regions (about 0.1 ppm at 600 MHz), we can put a lower limit on the rate of interconversion between helical and extended conformations in Δ131Δ of about 100 s^{-1}.

In order to estimate the fraction of helical conformation for each residue, we assume that the Hα chemical shift values for helical residues in native nuclease (Wang et al., 1992) correspond to 100% helix and that those in Gly-Gly-X-Ala model peptides correspond to 0% helix. We can use the formula:

$$f(\text{helix, \%}) = \frac{[\delta(\Delta131\Delta) - \delta(\text{random coil})]}{[\delta(\text{native nuclease}) - \delta(\text{random coil})]} \quad (2)$$

to calculate a helix fraction for each residue. If we average these values over all residues that are found in helical structure in the native state, we obtain a rough estimate of the fraction of α-helix conformers in Δ131Δ. The calculations based on Hα shifts give 27% helix for helix 2, 16% helix for helix 1, and 10% helix for helix 3 (Figure 1). The corresponding values calculated from the coil Cα chemical shifts (Wishart et al., 1991) and corrected for the mean 1.45 ppm offset are as follows: 34% helix for helix 2, 6% helix for helix 1, and 0% helix for helix 3. It should be emphasized that these values are only rough estimates. There is independent evidence, however, that the helical segments in Δ131Δ have dissimilar

stabilities. Thus, helix 1 gives weaker $d_{NN}(i,i+1)$ and $d_{\alpha\beta}(i,i+3)$ NOEs than helix 2. In addition, differences in HN temperature factors from random coil values are less pronounced for helix 1 than for helix 2 (Figure 7). The C-terminal helix 3 shows little evidence for helical structure except slightly raised C′ and slightly lowered Hα shift indices, respectively, and one $d_{\alpha N}(i,i+3)$ NOE between S128 and Q131.

Reverse-Turn Structure. Two stretches of residues which form reverse turns in the native state (83–86 and 94–97) give strong evidence for turn structure in Δ131Δ. These putative turns were initially identified by the unusually small $\Delta\delta/\Delta T$ (HN) factors for the residues in the fourth position of the turn: G86 (−4.0 ppb/K) and K97 (−2.6 ppb/K). Additional strong $d_{NN}(3,4)$, weak $d_{NN}(2,4)$ and $d_{\alpha N}(2,4)$ NOEs confirmed the turn assignment in each case. The geometries of different types of reverse turns can be distinguished from $^3J_{HN\text{-}H\alpha}$ values of the residues in positions 2 and 3. Due to spectral overlap in Δ131Δ, it was only possible to obtain $^3J_{HN\text{-}H\alpha}$ values for the residue in position 3 of both turns: 8.8 Hz for Y85, 5.8 Hz and 5.9 Hz for G96. These represent some of the few residues in Δ131Δ which do not show $^3J_{HN\text{-}H\alpha}$ values characteristic of averaging, indicating a significant preference for turn conformers. The $^3J_{HN\text{-}H\alpha}$ values are most consistent with a type-I turn for residues 83–86 (9 Hz for position 3 in an idealized turn) and with a type-I′ or type-II turn (5 Hz for position 3) for residues 94–97. In the native state, residues 83–86 form a type-I turn while residues 94–97 form a type-I′ turn. The 83–86 turn, at least, is thus completely consistent with the corresponding turn in the native state.

Turn conformations do not appear to be significantly populated for residues 52–55 and 115–118 by any of the criteria above. The absence of the *cis*-Pro-type VIa turn for residues 115–118 is not surprising, since this turn requires a substantially folded structure for stability (Evans et al., 1989; Alexandrescu et al., 1990; Raleigh et al., 1992; Hodel et al., 1993). Similarly, the concentrations of *cis* isomers were too low to detect for any of the four remaining Pro residues in Δ131Δ. There are insufficient assignment data to determine the geometries of residues which are involved in the other turns in native nuclease: 19–22, 27–30, 46–49 and 119–122.

β-Sheet Structure and Dynamics. The NMR data for Δ131Δ show little evidence for stable β-sheet structure. Fractional populations calculated from Hα shifts (eq 2) for the assigned residues in Δ131Δ that are in β-sheet structure in the native state are as follows: −24% for residues 24–27 (strand 2), −8% for residues 29–33 (strand 3), −1% for residues 71–76 (strand 4), and 15% for residues 91–94 (strand 5). The values calculated based on Cα chemical shifts are as follows: 12% for residues 24–27 (strand 2), 5% for residues 71–76 (strand 4), and −5% for residues 91–94 (strand 5). Negative fractional populations indicate that chemical shifts in Δ131Δ are closer to those expected for α-helix than for β-sheet. Strand 5 gives some Hα chemical shift values characteristic of β-sheet, but these are not supported by NOE data characteristic of β-sheet structure. Only one weak $d_{\alpha\alpha}$ NOE was detected in NOESY spectra of Δ131Δ, and it has not been possible to assign. Of the five strands in the nuclease β-barrel, some of the residues in both strands 4 (E73–E75) and 5 (A90–Y91) show medium $d_{NN}(i,i+1)$ NOEs (Figure 8), which are more indicative of turn or helix structure than β-sheet. Furthermore, $^3J_{HN\text{-}H\alpha}$ values, except for Y91 (9.2 Hz), are closer to coil values (7.5 Hz) than to β-sheet values (9 Hz). Strands 1–3 of the β-barrel occur near the N-terminus of Δ131Δ, which as mentioned above gives significantly poorer NMR data than the rest of the molecule. We cannot, therefore, rule out the presence of β-sheet structure in the N-terminal part of Δ131Δ. Furthermore, since α-helical structure in Δ131Δ shows substantial conformational averaging, it is not unreasonable to expect β-sheet structure in Δ131Δ to be subject to the same type of averaging. In the presence of comparable levels of conformational averaging, β-sheet structure may be considerably more difficult to detect than α-helix structure. With the exception of $d_{\alpha\alpha}$ NOEs, NMR parameters for extended coil and β-sheet conformations are roughly similar [e.g., large $^3J_{HN\text{-}H\alpha}$ values, strong $d_{\alpha N}(i+1)$ NOEs].

Tertiary Structure and Dynamics. One of the central issues in the characterization of partially folded proteins is the role of long-range tertiary interactions. At the current level of characterization, it is difficult to establish the extent and stability of tertiary structure in Δ131Δ. It is clear, however, that tertiary structure will be much more difficult to analyze than secondary structure in Δ131Δ: (1) Chemical shift dispersion is significantly smaller for side-chain than for backbone resonances. (2) Motional averaging of side chains is likely to be more unrestrained than the backbone (as is the case with native proteins), which is likely to cause large reductions in the intensities of long-range NOEs. In the presence of poor chemical shift dispersion and averaging, any putative NOE effect must be interpreted with great care. Thus, in the 3D $^1H\{^{15}N\}$NOESY-HMQC spectrum, at least 10 cross-peaks could not be attributed to interactions between residues close together in the sequence. Spectral overlap, however, is too severe to unambiguously assign these NOEs. The longest range NOE that could be identified with confidence in Δ131Δ is a weak NOE between the HN protons of E52 and E43, nine positions apart in the sequence. This NOE was detected both in 3D $^1H\{^{15}N\}$NOESY-HMQC and in 3D $^1H\{^{15}N\}$HSQC-NOESY-HSQC spectra and corresponds to a native-state distance of 5.0 Å. The assignment of this NOE was possible because both E52 and E43 give distinct HN and ^{15}N chemical shifts (Figure 3). Neither E52 nor E43 are involved in regular secondary structure in the native protein; E43, however, is the catalytic base in native nuclease.

A recurrent theme in the NMR of partially folded proteins is the severe broadening of resonances due to conformational averaging on the millisecond time scale [e.g., Jeng & Englander (1991)]. This line broadening often occurs for precisely those residues which are most likely to be involved in long-range tertiary interactions; for example, the hydrophobic box residues in the molten globule of α-lactalbumin (Baum et al., 1989; Alexandrescu et al., 1993). In the present case, this type of averaging may account for the weaker H–N correlation peaks for residues in the first three strands of β-sheet. An alternative possibility is that the intensity of amide residues in the first 40 residues of Δ131Δ is quenched by solvent exchange. We feel the latter is unlikely, since at pH 5.3 and a temperature of 32 °C even residues in a random coil conformation should exhibit solvent exchange at rates considerably slower than amide proton spin-lattice relaxation rates. Furthermore, HSQC spectra with water suppressed either by presaturation or by Messerle spin-lock pulses (Messerle et al., 1989) show little difference in either the number of the relative intensity of cross-peaks. In general, the presence of line broadening severely limits the application of NMR to conformational analysis of partially folded proteins, at least with the field strengths currently available. It would be of some advantage, therefore, to have a spectrum of partially folded proteins in which tertiary structure is more ordered than in Δ131Δ or than in the molten globules of some other proteins. Some model systems of this type are already available for nuclease:

(1) In the full-length protein, a set of mutations far removed in sequence from Pro 117 affect the cis/trans equilibrium at this site through the destabilization of tertiary interactions (Alexandrescu et al., 1990). (2) The 1–136 fragment of nuclease with the wild-type sequence has properties similar to Δ131Δ (Flanagan et al., 1992). While mutations such as V66L and G88V destabilize the native state of full-length nuclease, in the 1–136 fragment the same mutations appear to stabilize native-like structure (Shortle & Abeygunawardana, 1993). These types of model systems could provide important information about the interactions which play a role in stabilizing structure at intermediate or late stages in folding.

Implications for the Folding of Nuclease. The Δ131Δ fragment gives less NMR resonance dispersion and, in general, sharper lines than the "molten globule" intermediates of proteins such as α-lactalbumin (Alexandrescu et al., 1993), cytochrome *c* (Jeng & Englander, 1991), and a 1–136 fragment of nuclease containing the structure-stabilizing mutation G88V (Shortle & Abeygunawardana, 1993). Furthermore, Δ131Δ appears to be less compact by small angle X-ray scattering and by gel filtration than would be expected for a molten globule of this protein (D. Shortle and M. Kataoka, unpublished results), gives less negative ellipticity in the peptide region of the CD spectrum than the native protein, and affords no detectable protection[3] of amide protons from solvent exchange at pH 5.3. Taken together, these observations suggest that the Δ131Δ fragment represents a conformational ensemble which is much less structured than that of a molten globule.

It has been noted that equilibrium molten globules share many of the properties of transient intermediates which occur at early stages during the folding reaction (Kuwajima, 1989, Ptitsyn, 1991). It is interesting that early kinetic intermediates in nuclease contain less stable structure than kinetic intermediates of proteins which form stable equilibrium molten globules. Thus, only 30% of the native-state peptide ellipticity is regained during the first stages of nuclease folding compared to 80% for α-lactalbumin (Sugawara et al., 1991). The fast chemical shift averaging between helical and extended conformations in Δ131Δ suggests that the α-helices in Δ131Δ are formed and disrupted on time scales shorter than 10 ms. These helices should, therefore, be present at the earliest stages of the folding reaction and may be interconnected to the changes in peptide CD spectra obtained during the 15-ms dead-time of stopped-flow urea-refolding experiments of nuclease (Sugawara et al., 1991). Furthermore, since protein synthesis is slower than folding (Anfinsen, 1973), it is possible that the type of structure observed in these studies may be present in nascent protein chains before they leave the ribosome.

The most persistent structures identified in Δ131Δ are highly similar to elements of secondary structure found in the native state, albeit with greatly reduced stability. There is evidence for residual α-helix structure for segments of the chain which form helix 2 and helix 1 in the native state. Residues 83–86 and possibly 94–97 are present in native-like reverse-turn conformations in Δ131Δ. This similarity extends to a long-range NOE identified between the HN protons of E43 and E52, which is also consistent with the native-state structure. The presence of considerable native-like secondary structure is highly suggestive of a "hierarchical" folding model, in which elements of localized structure "flicker in and out of the conformation that they occupy in the final protein" (Anfinsen, 1973). The native-like properties of these structures suggest that they play a role in limiting the volume of conformational space that need be explored during subsequent stages of folding (Ptitsyn, 1991). Future studies of nuclease under conditions that permit increasing amounts of residual structure may define an equilibrium folding pathway that reflects the hierarchy of steps of native structure assembly.

[3] We did not attempt to study solvent exchange in the pH range 3.0–2.0, the optimal pH for exchange studies, as CD spectroscopy suggests a further unfolding of the residual structure in the Δ131Δ fragment in this pH range.

ACKNOWLEDGMENT

We thank Alan Meeker for preparation of a $^{15}N/^{13}C$-labeled protein sample and Arthur Edison, Dr. Milo Westler, and Dr. Ed. Mooberry for help and advice in setting up the 3D HSQC-NOESY-HSQC experiment. The $^{1}H\{^{15}N\}$HMQC-*J* and HSQC-NOESY-HSQC experiments described in this paper were collected at NMRFAM in Madison during a quench of the AM600 machine at Johns Hopkins USM.

SUPPLEMENTARY MATERIAL AVAILABLE

Assignment table summarizing ^{1}H, ^{15}N, $^{13}C_{\alpha}$, and $^{13}C'$ chemical shifts for the assigned resonances in Δ131Δ; table of NMR experiments used to assign and analyze Δ131Δ including sizes, sweep widths, and digital resolution of raw and processed NMR data matrices; figures showing representative planes from 3D $^{1}H\{^{15}N\}$TOCSY-HMQC and 3D HNCA data sets; figure summarizing the sequential connectivity information used to obtain sequence specific NMR assignments for Δ131Δ (10 pages). Ordering information is given on any current masthead page.

REFERENCES

Alexandrescu, A. T., Hinck, A. P., & Markley, J. L. (1990) *Biochemistry 29*, 4516–4525.
Alexandrescu, A. T., Evans, P. A., Pitkeathly, M., Baum, J., & Dobson, C. M. (1993) *Biochemistry 32*, 1707–1718.
Alexandrescu, A. T., Ng, Y.-L., & Dobson, C. M. (1994) *J. Mol. Biol.* (in press).
Anfinsen, C. B. (1973) *Science 181*, 223–230.
Baum, J., Dobson, C. M., Evans, P. A., & Hanley, C. (1989) *Biochemistry 28*, 7–13.
Bax, A., & Ikura, M. (1991) *J. Biomol. NMR 1*, 99–104.
Bax, A., Ikura, M., Kay, L. E., Torchia, D. A., & Tschudin, R. (1990) *J. Magn. Reson. 86*, 304–318.
Dill, K. A., & Shortle, D. (1991) *Annu. Rev. Biochem. 60*, 795–825.
Dobson, C. M. (1992a) *Curr. Opin. Struct. Biol. 2*, 6–12.
Dobson, C. M. (1992b) *Curr. Opin. Struct. Biol. 2*, 343–345.
Dyson, H. J., & Wright, P. E. (1991) *Annu. Rev. Biophys. Biophys. Chem. 20*, 519–538.
Evans, P. A., Kautz, R. A., Fox, R. O., & Dobson, C. M. (1989) *Biochemistry 28*, 362–370.
Fan, P., Bracken, W. C., & Baum, J. (1993) *Biochemistry 32*, 1573–1582.
Flanagan, J. M., Kataoka, M., Shortle, D., & Engelman, D. M. (1992) *Proc. Natl. Acad. Sci. U.S.A. 89*, 748–752.
Gronenborn, A. M., Bax, A., Wingfield, P. T., & Clore, G. M. (1989) *FEBS Lett. 243*, 93–98.
Hodel, A., Kautz, R. A., Jacobs, M. D., & Fox, R. O. (1993) *Protein Sci. 2*, 838–850.
Jeng, M., & Englander, S. W. (1991) *J. Mol. Biol. 221*, 1045–1061.
Kay, L. E., & Bax, A. (1990) *J. Magn. Reson. 86*, 110–126.
Kay, L. E., Marion, D., & Bax, A. (1989) *J. Magn. Reson. 84*, 72–84.

Kay, L. E., Ikura, M., Tschudin, R., & Bax, A. (1990) *J. Magn. Reson. 89*, 496–514.
Kunkel, T. A. (1985) *Proc. Natl. Acad. Sci. U.S.A. 82*, 488–492.
Kuwajima, K. (1989) *Proteins: Struct., Funct., Genet. 6*, 87.
Levy, G. C., & Lichter, R. L. (1979) *Nitrogen-15 Nuclear Magnetic Resonance Spectroscopy*, John Wiley & Sons, New York.
Logan, T. M., Olejniczak, E. T., Xu, R. X., & Fesik, S. W. (1993) *J. Biomol. NMR 3*, 225–231.
Loll, P. J., & Lattman, E. E. (1989) *Proteins: Struct., Funct., Genet. 5*, 183–201.
Marion, D., Driscoll, P. C., Kay, L. E., Wingfield, P. T., Bax, A., Gronenborn, A. M., & Clore, G. M. (1989a) *Biochemistry 28*, 6150–6156.
Marion, D., Ikura, M., & Bax, A. (1989b) *J. Magn. Reson. 85*, 393–399.
Messerle, B. A., Wider, G., Otting, G., Weber, C., & Wüthrich, K. (1989) *J. Magn. Reson. 85*, 608–613.
Neri, D., Wider, G., & Wüthrich, K. (1992a) *Proc. Natl. Acad. Sci. U.S.A. 89*, 4397–4401.
Neri, D., Billeter, M., Wider, G., & Wüthrich, K. (1992b) *Science 257*, 1559–1563.
Ptitsyn, O. B. (1991) *FEBS Lett. 285*, 176–181.
Raleigh, D. P., Evans, P. A., Pitkeathly, M., & Dobson, C. M. (1992) *J. Mol. Biol. 228*, 338–342.
Redfield, C., & Dobson, C. M. (1988) *Biochemistry 27*, 122–136.
Serpersu, E. H., Shortle, D., & Mildvan, A. K. (1986) *Biochemistry 25*, 68–77.
Shortle, D. (1993) *Curr. Opin. Struct. Biol. 3*, 66–74.
Shortle, D., & Meeker, A. K. (1989) *Biochemistry 28*, 936–944.
Shortle, D., & Abeygunawardana, C. (1993) *STRUCTURE 1*, 121–134.
Shortle, D., Stites, W. E., & Meeker, A. K. (1990) *Biochemistry 29*, 8033–8041.
Spera, S., & Bax, A. (1991) *J. Am. Chem. Soc. 113*, 5490.
Stockman, B. J., Euvrard, A., & Scahill, T. A. (1993) *J. Biomol. NMR 3*, 285–296.
Sugawara, T., Kuwajima, K., & Sugai, S. (1991) *Biochemistry 30*, 2698–2706.
van Mierlo, C. P. M., Darby, N. J., Keeler, J., Neuhaus, D., & Creighton, T. E. (1993) *J. Mol. Biol. 229*, 1125–1146.
Wang, J., Hinck, A. P., Loh, S. N., LeMaster, D. M., & Markley, J. L. (1992) *Biochemistry 31*, 921–936.
Wishart, D. S., Sykes, B. D., & Richards, F. M. (1991) *J. Mol. Biol. 222*, 311–333.
Wüthrich, K. (1986) *NMR of Proteins and Nucleic Acids*, John Wiley & Sons, Inc., New York.